Journal of Pharmacological Sciences 129 (2015) 143–149

HOSTED BY

ELSEVIER

Contents lists available at ScienceDirect

Journal of Pharmacological Sciences

journal homepage: www.elsevier.com/locate/jphs

Full paper

Mg^{2+}-dependent facilitation and inactivation of L-type Ca^{2+} channels in guinea pig ventricular myocytes

Meimi Zhao [a, b], Rui Feng [a, b], Dongxue Shao [a], Shuyuan Liu [a], Ming Lei [a], Hongmei Wang [a], Xuefei Sun [a, b], Feng Guo [a, b], Huiyuan Hu [a, b], Masaki Kameyama [c], Liying Hao [a, b, *]

[a] Department of Pharmaceutical Toxicology, School of Pharmacy, China Medical University, Shenyang 110122, China
[b] Cardiovascular Institute of China Medical University, Shenyang 110001, China
[c] Department of Physiology, Graduate School of Medical and Dental Sciences, Kagoshima University, Kagoshima 890-8544, Japan

ARTICLE INFO

Article history:
Received 11 February 2015
Received in revised form
31 July 2015
Accepted 3 August 2015
Available online 7 August 2015

Keywords:
Mg^{2+}
Ca^{2+} channels
Open probability
Open time
Inside-out configuration

ABSTRACT

This study aimed to investigate the intracellular Mg^{2+} regulation of the L-type Ca^{2+} channels in guinea pig ventricular myocytes. By adopting the inside-out configuration of the patch clamp technique, single channel currents of the L-type Ca^{2+} channels were recorded at different intracellular Mg^{2+} concentrations ($[Mg^{2+}]_i$). At free $[Mg^{2+}]_i$ of 0, 10^{-9}, 10^{-7}, 10^{-5}, 10^{-3}, and 10^{-1} M, 1.4 μM CaM + 3 mM ATP induced channel activities of 44%, 117%, 202%, 181%, 147%, and 20% of the control activity in cell-attached mode, respectively, showing a bell-shaped concentration-response relationship. Moreover, the intracellular Mg^{2+} modulated the Ca^{2+} channel gating properties, accounting for alterations in channel activities. These results imply that Mg^{2+} has a dual effect on the L-type Ca^{2+} channels: facilitation and inhibition. Lower $[Mg^{2+}]_i$ maintains and enhances the basal activity of Ca^{2+} channels, whereas higher $[Mg^{2+}]_i$ inhibits channel activity. Taken together, our data from the application of an $[Mg^{2+}]_i$ series suggest that the dual effect of Mg^{2+} upon the L-type Ca^{2+} channels exhibits long open-time dependence.

1. Introduction

Voltage-gated Ca^{2+} channels mediate Ca^{2+} entry into cells in response to membrane depolarization. The Ca^{2+} channels can be divided into high-voltage-activated (L, N, P/Q, and R-types) and low-voltage-activated (T-type) Ca^{2+} channels. They have been biochemically characterized, revealing their existence as a complex consisting of a pore-forming α1 subunit of approximately 190–250 kDa, a transmembrane, disulfide-linked complex of α2 and δ subunits, an intracellular β subunit, and in some cases, a transmembrane γ subunit. The α1 subunit is encoded by three gene families: Ca_v1 (L-type Ca^{2+} channels), Ca_v2 (N, P/Q, and R-type Ca^{2+} channels), and Ca_v3 (T-type Ca^{2+} channels). More specifically, the Ca_v1 family contains several sub-types, which consequently denote their corresponding channel sub-types: $Ca_v1.1$ (α1S) is expressed in mammalian skeletal muscle, $Ca_v1.2$ (α1C) is expressed in the heart and brain, and $Ca_v1.3$ (α1D) is expressed in the kidneys and endocrine tissue (1). Functionally, activation of the L-type Ca^{2+} channels initiates muscle contraction, excitation-contraction coupling, endocrine secretion, and gene transcription (1). The blocking of L-type Ca^{2+} channels by clinically used Ca^{2+} channel blockers (such as nifedipine, amlodipine, verapamil, and diltiazem) explains most of the therapeutic effects of these drugs, such as lowering of blood pressure and improvement in conditions that can otherwise lead to myocardial infarction and arrhythmia (2).

L-type Ca^{2+} channels contain multiple binding sites for divalent cations such as Ca^{2+} and Mg^{2+}, which allow intracellular Ca^{2+} and Mg^{2+} to regulate the Ca^{2+} channel at physiological concentrations (3–5). The intracellular Ca^{2+} concentration ($[Ca^{2+}]_i$) is ~100 nM whilst the extracellular Ca^{2+} concentration is ~2 mM, forming a steep concentration gradient that favors voltage-gated Ca^{2+} influx when cell membrane excitation is stimulated. The increased intracellular Ca^{2+} induced by Ca^{2+} influx modulates the Ca^{2+} channels by the mechanisms known as Ca^{2+}-dependent facilitation (CDF) and inactivation (CDI) (1).

* Corresponding author. Department of Pharmaceutical Toxicology, School of Pharmacy, China Medical University, Shenyang 110122, China.
E-mail address: lyhao@mail.cmu.edu.cn (L. Hao).
Peer review under responsibility of Japanese Pharmacological Society.

http://dx.doi.org/10.1016/j.jphs.2015.08.001

Magnesium ions, as the most abundant divalent cation in the internal milieu, also play important roles in living cells, including as a cofactor for enzymatic reactions, stabilizing protein structures, and blocking Ca^{2+}/K^{+} channels (6). However, the mechanism underlying the regulatory effects of Mg^{2+} on intracellular signaling transduction systems has not yet been fully understood (7), perhaps due to the absence of large fluctuations in intracellular Mg^{2+} concentration ($[Mg^{2+}]_i$) in the cardiovascular system and a present lack of any effective techniques to measure $[Mg^{2+}]_i$ in subcellular regions. On the other hand, clinically, Mg^{2+} has been shown to be an effective therapeutic agent (8,9) in the treatment of many diseases, such as eclampsia and T-cell immunodeficiency. In particular, Mg^{2+} supplements are thought to be an effective therapy in the prevention, management, and even in the treatment of cardiovascular diseases (CVDs) such as arrhythmia (10), hypertension (11), or heart failure (12). Given the importance of the L-type Ca^{2+} channels in cardiac function, Mg^{2+} modulation of the channels may play a significant role in these CVD-associated pathophysiological processes.

Previous studies have confirmed the marked inhibitory actions of increased Mg^{2+} concentration on I_{Ca}. A study of the effects of Mg^{2+} on the Ca^{2+} currents (I_{Ca}) in frog myocytes showed that increasing $[Mg^{2+}]_i$ between 0.3 and 3 mM caused a decrease in I_{Ca} by more than 50% (13). Both the groups of Catterall and of Berlin have focused on the mechanisms that underlie regulation of the L-type Ca^{2+} channels by Mg^{2+}, at $[Mg^{2+}]_i$ between 0.1 and 10 mM (14–19). Their studies showed marked inhibitory effects on I_{Ca} around physiologically relevant $[Mg^{2+}]_i$ of 0.3–1.3 mM (8,20–22). In addition, Brunet et al. considered the Ba^{2+} current (I_{Ba}) and examined I_{Ca}/I_{Ba} via the L-type Ca^{2+} channels over a range of $[Mg^{2+}]_i$, from 0.1 to 7.2 mM (18), and found that the data could be described by a one-binding-site model. On the other hand, low Mg^{2+} concentration can lead to arrhythmia in which I_{Ca} plays an important role. However, the changes in I_{Ca} under conditions of $[Mg^{2+}]_i$ lower than physiological levels are still unknown.

The mechanism responsible for Mg^{2+} modulation of I_{Ca} in cardiac cells is controversial, but several alternatives have been proposed. One possible mechanism is a direct pore block by external Mg^{2+} (23), the other is an indirect mode of interaction of internal Mg^{2+} via modification of the activities of protein kinases or phosphoprotein phosphatases (13,19,24). It is also suggested that an internal Mg^{2+} may induce a change in channel gating kinetics. Yamaoka and Seyama first reported that Mg^{2+} acts upon channel gating properties (25). Recently, Wang and Berlin discussed channel gating kinetics as a compelling explanation for these results (17). However, direct experimental support for this mechanism remains elusive.

The purpose of this study was to investigate the $[Mg^{2+}]_i$-induced modulation of the L-type Ca^{2+} channels over a wider range of $[Mg^{2+}]_i$ than had been considered previously: from 0 to 100 mM, covering concentrations close to and far from physiological levels. In the present study, we employed calmodulin (CaM) and ATP to prevent "rundown" of cardiac L-type Ca^{2+} channels (26–28), which enabled us to analyze the effect of Mg^{2+} on the I_{Ba} through the Ca^{2+} channel, under conditions where control of the $[Mg^{2+}]_i$ was feasible. We found that intracellular Mg^{2+} has a dual effect on the regulation of L-type Ca^{2+} channels activities: facilitation and inactivation.

2. Materials and methods

2.1. Animals

Adult, healthy guinea pigs, weighing 250–350 g, were purchased from the animal center of China Medical University. All animals were housed in clear cages with ad libitum access to food and water, and a 12 h light/dark cycle. The surgery was performed under sodium pentobarbital anesthesia, and all efforts were made to minimize suffering. This study was carried out in strict accordance with the recommendations of the Guide for the Care and Use of Laboratory Animals of the National Institutes of Health.

2.2. Solutions and chemicals

Tyrode solution was used as the standard solution for isolating guinea pig ventricular myocytes. Tyrode solution was composed of (all concentrations listed have units of mM, unless otherwise stated) NaCl 135, KCl 5.4, NaH_2PO_4 0.33, $MgCl_2$ 1, glucose 5.5, $CaCl_2$ 1.8, and 4-(2-hydroxyethyl)-1-piperazineethanesulfonic acid (HEPES)–NaOH buffer 10 (pH 7.4). Ca^{2+}-free Tyrode solution had $CaCl_2$ excluded. Ca^{2+}-free Tyrode solution containing 0.25 mg/ml collagenase type I (Worthington, NJ, USA) was used as the collagenase solution for digesting single guinea pig ventricular myocytes. Kraftbrühe-modified (KB) solution was used as a storage solution for ventricular cells and contained (mM) KOH 70, glutamic acid 50, KCl 40, taurine 20, KH_2PO_4 20, glucose 10, EGTA 0.5, $MgCl_2$ 3, and HEPES–KOH buffer 10 (pH 7.4).

To record the unitary I_{Ba} via the L-type Ca^{2+} channels, in guinea pig ventricular myocytes, a pipette solution and basic internal solution were used. The pipette solution contained the following components (mM): $BaCl_2$ 50, tetraethylammonium chloride (TEA Cl) 70, EGTA 0.5, Bay K8644 0.003 and HEPES–CsOH buffer 10 (pH 7.4). The supplement of Bay K8644 0.003 in the pipette solution was to enhance the open-state probability of L-type Ca^{2+} channels (29–31). The basic internal solution consisted of (mM): aspartic acid 120, KOH 120, KCl 30, $MgCl_2$ 0.5, EGTA 1, $CaCl_2$ 0.5, and HEPES–KOH buffer 10 (pH 7.4). According to our previous reports (26–28), CaM (1.4 μM) + ATP (3 mM) were added in the basic internal solution when Ca^{2+} channel activity was recorded in the inside-out configuration to prevent rundown of the channel activity. To examine the effects of different free $[Mg^{2+}]_i$ while maintaining constant Ca^{2+} and other ion concentrations, MaxChelator software (website: http://maxchelator.stanford.edu/) was used to calculate the total and free concentrations of $MgCl_2$ and $CaCl_2$ to obtain pCa = 7 and pH = 7.2 at room temperature. The composition of these solutions is shown in Table 1.

Escherichia coli BL21 was transformed with the CaM-cDNA-inserted pGEX6P plasmid (27). The expression of glutathione *S*-transferase (GST) fusion protein of CaM was induced by isopropyl-β-D-1-thiogalactopyranoside (IPTG), and purified using glutathione Sepharose 4B (GE Healthcare, NJ, USA). PreScission Protease (GE Healthcare, NJ, USA) was used to remove the GST region of CaM. Finally, we detected CaM expression levels by SDS-PAGE and quantified these levels by the Bradford method. CaM was kept in the basic internal solution used for patch-clamp electrophysiology.

2.3. Ventricular myocyte isolation

Single ventricular cells were obtained from adult guinea pig hearts by enzymatic dispersion, as described previously (32). Briefly, the isolated heart was mounted on Langendorff apparatus to carry out aortic retrograde perfusion. Tyrode solution, Ca^{2+}-free Tyrode solution, and collagenase solution were perfused for 3, 6, and 10–15 min, respectively, at 37 °C. The collagenase solution was then washed with KB solution. Finally, the left ventricle tissue was cut into pieces and filtered through a 105-μm stainless-steel mesh filter. The obtained single ventricular myocytes were maintained in the KB solution, at 4 °C, until use.

2.4. Patch-clamp electrophysiology

Electrophysiology using inside-out single-channel patch mode was carried out according to published methods (27). Single I_{Ca}

Table 1
Composition of internal solutions. All values have units of millimolar (mM). Ion concentrations were calculated with Ca–Mg–ATP–EGTA calculator v1.0 which is available from the Stanford University website (http://maxchelator.stanford.edu/), using their stability constants. CaM: calmodulin, $[Mg^{2+}]_i$: intracellular Mg^{2+} concentration, $[Ca^{2+}]_i$: intracellular Ca^{2+} concentration.

Free $[Mg^{2+}]_i$	0	10^{-9} M	10^{-7} M	10^{-5} M	10^{-3} M	10^{-1} M
	Total component concentrations					
$MgCl_2$	0	0.00003	0.0025	0.24	3.7	103.7
$CaCl_2$	0.46	0.46	0.46	0.46	0.45	0.10
Aspartic acid	120	120	120	120	120	120
KOH	120	120	120	120	120	120
KCl	30	30	30	30	30	30
EGTA	1	1	1	1	1	1
CaM	0.0014	0.0014	0.0014	0.0014	0.0014	0.0014
K_2ATP	3	3	3	3	3	3
	Calculated ion concentrations					
pH	7.4	7.4	7.4	7.4	7.4	7.4
EGTA	1	1	1	1	1	1
ATP	3	3	3	3	3	3
Free $[Mg^{2+}]_i$	0	0.000001	0.0001	0.01	1	100
Free $[Ca^{2+}]_i$	0.0001	0.0001	0.0001	0.0001	0.0001	0.0001
Free EGTA	0.539	0.539	0.539	0.539	0.522	0.154
Free ATP	2.998	2.998	2.996	2.771	0.326	0.007

were recorded using the patch-clamp technique at room temperature (23–25 °C) using a patch pipette (2–4 MΩ). After recording the Ca^{2+} channel activity in cell-attached mode for 2 min, the membrane patch was excised to establish an inside-out patch configuration (represented as i.o. in the figures). One minute later, the clamped patches were moved into a small inset in the perfusion chamber and test solutions were applied, containing different Mg^{2+} concentrations. Unitary Ba^{2+} currents (I_{Ba}) through the Ca^{2+} channels were elicited by depolarizing pulses, from −70 mV to 0 mV, for 200-ms duration, at a rate of 0.5 Hz, recorded with a patch clamp amplifier (Axopatch 200B, Axon Instruments, USA), and they were then fed to a computer at a sampling rate of 3.3 kHz after being filtered at 1 kHz.

2.5. Data analysis

In the analysis of single-channel events, a computer program (Clampfit 10.0, Axon Instruments, USA) was used. Since the mean current (*I*) is a product of the number (*N*), the time-averaged open-state probability (*Po*), and the unitary current amplitude (*i*), of channels in the patch, channel activity (*NPo*) was equal to *I* divided by *i*. The relative channel activity, used as a further channel activity parameter, was represented as the *NPo* ratio obtained from the inside-out patch and the cell-attached patch, when using the same patch; in the other words, this parameter eliminated the differences in channel activity before the intracellular Mg^{2+} treatment. We analyzed the open time by using current traces filtered at 1 kHz, and compiled the data into histograms with equal bin widths of 2 ms.

Data were presented as means ± standard error (SE). Statistical significance between groups was calculated by unpaired two-tailed Student's *t*-test, and $P < 0.05$ was considered significant.

3. Results

3.1. Mg^{2+} concentration-dependent facilitation of Ca^{2+} channel activities

Previous studies have characterized the Mg^{2+} dependence of cardiac I_{Ca} in the whole-cell configuration and showed that I_{Ca} is inhibited by intracellular Mg^{2+} over a concentration range of 0.1–10 mM (13–19). Despite the availability of evidence that explains the modulation of the L-type Ca^{2+} channels by free intracellular Mg^{2+} as a transduction message at the physiological level, the effects of intracellular Mg^{2+} depletion or very high Mg^{2+} concentrations remain elusive. We employed the inside-out configuration of the single patch-clamp technique to investigate a wide range of $[Mg^{2+}]_i$ and their regulation of the L-type Ca^{2+} channels.

In our previous studies, we demonstrated that CaM (1.4 μM) + ATP (3 mM) reversed the rundown of the L-type Ca^{2+} channels in the inside-out patch at a free $[Ca^{2+}]_i$ of 0.1 μM (27). Adopting this method in our present study, we observed the effects of a series of $[Mg^{2+}]_i$ on single Ca^{2+} channel activity in guinea pig ventricular myocytes. We found that Mg^{2+} depletion or 10^{-1} M Mg^{2+} could not reverse the rundown of the L-type Ca^{2+} channels in the inside-out patch, as shown in Fig. 1A and F. Whereas, 10^{-9} to 10^{-3} M Mg^{2+} could reverse the rundown of L-type Ca^{2+} channels, to a certain extent (Fig. 1B–E).

3.2. Mg^{2+} concentration-dependent inactivation of Ca^{2+} channel activities

The highest channel activity, of ~202 ± 4% (n = 7), was induced at 10^{-7} M $[Mg^{2+}]_i$, as shown in Fig. 2. However, further increasing the $[Mg^{2+}]_i$ did not cause the channel activity to increase further. At $[Mg^{2+}]_i$ of 10^{-5} and 10^{-3} M, the channel activities were 181 ± 2% (n = 6) and 147 ± 1% (n = 6) respectively, showing a decline in the channel activity. When $[Mg^{2+}]_i$ was increased to 10^{-1} M, the channel activity decreased even further to 20 ± 1% (n = 7). On the other hand, at the low $[Mg^{2+}]_i$ of 0 and 10^{-9} M, the channel activities were as low as 44 ± 4% (n = 6) and 117 ± 1% (n = 6), respectively. Thus, the concentration-dependence of Mg^{2+} showed a clear, bell-shaped concentration-response relationship, implying that Mg^{2+} has a dual effect: facilitation and inhibition.

The $[Mg^{2+}]_i$ series was applied successively. We first observed that 10^{-5} M Mg^{2+} induced a channel activity of 182% relative to that recorded in the cell-attached mode at a free $[Ca^{2+}]_i$ of 0.1 μM. However, rather than inducing further increase in the channel activity, the subsequent application of 10^{-1} M Mg^{2+} only induced a small amount of channel activity (22%) (Fig. 3). These results provide further support for the conclusion that Mg^{2+} does have a dual effect.

3.3. Mg^{2+}-dependent mode 2 activity of the L-type Ca^{2+} channels

The mechanism by which Mg^{2+} regulates the L-type Ca^{2+} channels is still unclear. Recently, growing evidence has demonstrated that Mg^{2+} modulation of Ca^{2+} channel gating properties is likely to be an underlying mechanism (17,25). Therefore, we then

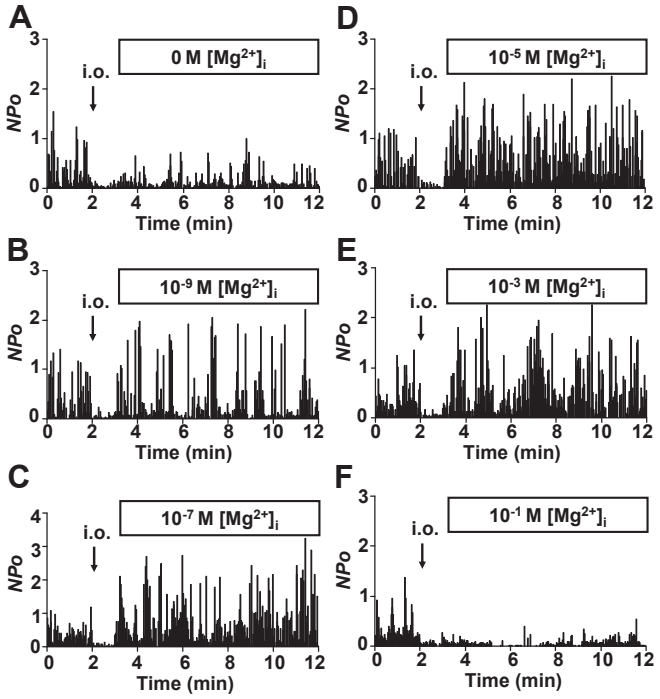

Fig. 1. Concentration-dependence of the Mg^{2+} effects on L-type Ca^{2+} channels. The effects of different intracellular Mg^{2+} concentrations $[Mg^{2+}]_i$ on the channel activities (*NPo*) were plotted against time. The pipettes contained 50 mM Ba^{2+} to enhance the single-channel conductance, and 3 μM Bay K8644 to increase the open-state probability (*Po*) of the L-type Ca^{2+} channels. The inside-out patch mode (i.o.) was initiated at the times indicated by arrows. The external solution contained 1.4 μM CaM and 3 mM ATP to prevent rundown of the L-type Ca^{2+} channels in the inside-out mode. $[Mg^{2+}]_i$ of 0 M (A), 10^{-9} M (B), 10^{-7} M (C), 10^{-5} M (D), 10^{-3} M (E), and 10^{-1} M (F), as indicated by the boxes, were administered together with 1.4 μM CaM and 3 mM ATP at an intracellular Ca^{2+} concentration $[Ca^{2+}]_i$ of 100 nM.

considered the functional effects of Mg^{2+} on the gating of L-type Ca^{2+} channels, in order to study the mechanisms by which changes in $[Mg^{2+}]_i$, between 0 and 10^{-1} M, might affect single Ca^{2+} channel activity.

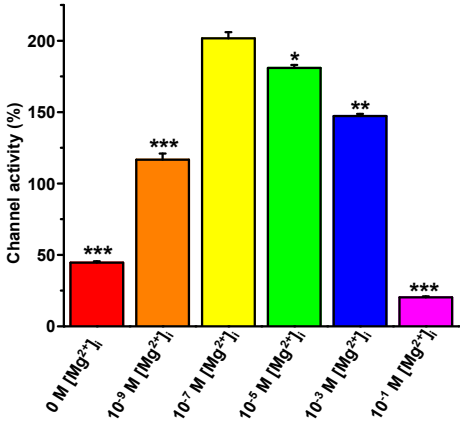

Fig. 2. Mg^{2+}-dependent facilitation and inactivation of Ca^{2+} channel activity. Summary of the mean relative channel activities recorded in the inside-out patch mode, with various intracellular Mg^{2+} concentrations $[Mg^{2+}]_i$ and a fixed intracellular Ca^{2+} concentration $[Ca^{2+}]_i$ of 100 nM. When $[Mg^{2+}]_i$ was 10^{-7} M, the channel activity reached maximal effect. After this point, higher $[Mg^{2+}]_i$ inhibited the channel activity in a dose-dependent manner. $^*P < 0.05$, $^{**}P < 0.01$, $^{***}P < 0.001$, versus 10^{-7} M $[Mg^{2+}]_i$ group. $n = 5–8$ in each group.

Quantification of the open times of single L-type Ca^{2+} channels is illustrated in Fig. 4. Open time histograms were best described by short (τ_{o1}) and long (τ_{o2}) open time constants. Addition of different $[Mg^{2+}]_i$ to the cytoplasmic face of the channels did not affect the duration of short open time but did alter the long open-time. At an $[Mg^{2+}]_i$ of 10^{-7} M, the τ_{o2} was the highest, at ~12.2 ± 0.7 ms (n = 3) (Fig. 5A). At higher $[Mg^{2+}]_i$, of 10^{-5}, 10^{-3} and 10^{-1} M, the τ_{o2} were 11.5 ± 0.5 ms (n = 3), 12.3 ± 0.5 ms (n = 3) and 9.4 ± 0.3 ms (n = 3), respectively, but only the 10^{-1} M Mg^{2+} group result was significantly low in comparison with the 10^{-7} M group. However, at lower $[Mg^{2+}]_i$, of 0 and 10^{-9} M, the τ_{o2} were 3.6 ± 0.4 ms (n = 3) and 6.9 ± 0.5 ms (n = 3) respectively, and both were significantly lower than the τ_{o2} for the 10^{-7} M Mg^{2+} group. On the other hand, At 10^{-7} M Mg^{2+}, the mode 2 frequency was the highest, at ~40 ± 1.7% (n = 3) (Fig. 5B). At higher $[Mg^{2+}]_i$, of 10^{-5}, 10^{-3} and 10^{-1} M, the mode 2 frequencies were 31 ± 2.2% (n = 3), 20 ± 1.4% (n = 3) and 4 ± 0.6% (n = 3), respectively, which were all significantly lower than the 10^{-7} M Mg^{2+} group. However, at lower $[Mg^{2+}]_i$, of 0 and 10^{-9} M, the mode 2 frequencies were 5 ± 0.5% (n = 3) and 16 ± 1.7% (n = 3) respectively, both of which were significantly lower than the frequency for the 10^{-7} M Mg^{2+} group. Thus, the data suggest that the effects of $[Mg^{2+}]_i$, between 0 and 10^{-1} M, are dependent on channel gating kinetics, especially mode 2 gating.

4. Discussion

In the present study, we have investigated the regulatory effects of intracellular Mg^{2+} on the L-type Ca^{2+} channels of isolated guinea pig ventricular myocytes in cell-free patches, where the concentration of Mg^{2+} in the intracellular surface of the membrane has been relatively finely controlled. Here, by constructing the concentration-response curve of Ca^{2+} channel activity versus intracellular Mg^{2+} concentration ($[Mg^{2+}]_i$), we confirmed that higher $[Mg^{2+}]_i$ inhibited Ca^{2+} channel activity, a result that is in agreement with an earlier study. More interestingly, for the first time, we have found that a certain level of intracellular Mg^{2+} was required to maintain the basal activity of Ca^{2+} channels, and an increase in the $[Mg^{2+}]_i$ from 0 to 10^{-7} M may enhance Ca^{2+} channel activity. Thus, the major finding of the present study is that Mg^{2+} exhibits a dual effect on the L-type Ca^{2+} channels: facilitation and inhibition.

The Mg^{2+}-induced Ca^{2+} channel facilitation occurred at a relatively lower $[Mg^{2+}]_i$ from 0 to 10^{-7} M. Since the fine control of $[Mg^{2+}]_i$ is not easy at levels less than the physiological level of Mg^{2+} (at least 0.3 mM) in the whole-cell Ca^{2+} current recording condition unless intracellular perfusion was used, the effects of Mg^{2+} at this low concentration range had not been well documented in previous studies. In present study, we employed the inside-out configuration for single channel recording, in which it was possible to control the $[Mg^{2+}]_i$ by changing the Mg^{2+} concentration of the perfusion solution (internal solution, see Table 1). When the $[Mg^{2+}]_i$ was free, there was no apparent Ca^{2+} channel activity, but when $[Mg^{2+}]_i$ was increased to 10^{-9} M, the channel opening was evident, with a relative channel activity of ~100% versus that in cell-attached mode, indicating that $[Mg^{2+}]_i$ 10^{-9} M was required to maintain the basal activity of the Ca^{2+} channels. Further increasing $[Mg^{2+}]_i$ from 10^{-9} to 10^{-7} M, the Ca^{2+} channel activity was shown to be ~200%, indicating that the channel was significantly facilitated by Mg^{2+}. A previous study by Lansman et al. has also reported the effects of external Mg^{2+} ($[Mg^{2+}]_o$) at zero concentration in cell-attached patch recordings from guinea pig ventricular cells (33). Their results showed that without $[Mg^{2+}]_o$, the single Ca^{2+} channel currents were at their highest. These opposing changes in Ca^{2+} channel activity caused by $[Mg^{2+}]_i$ and $[Mg^{2+}]_o$ may be the reason for the different mechanisms underlying Mg^{2+} regulation. For

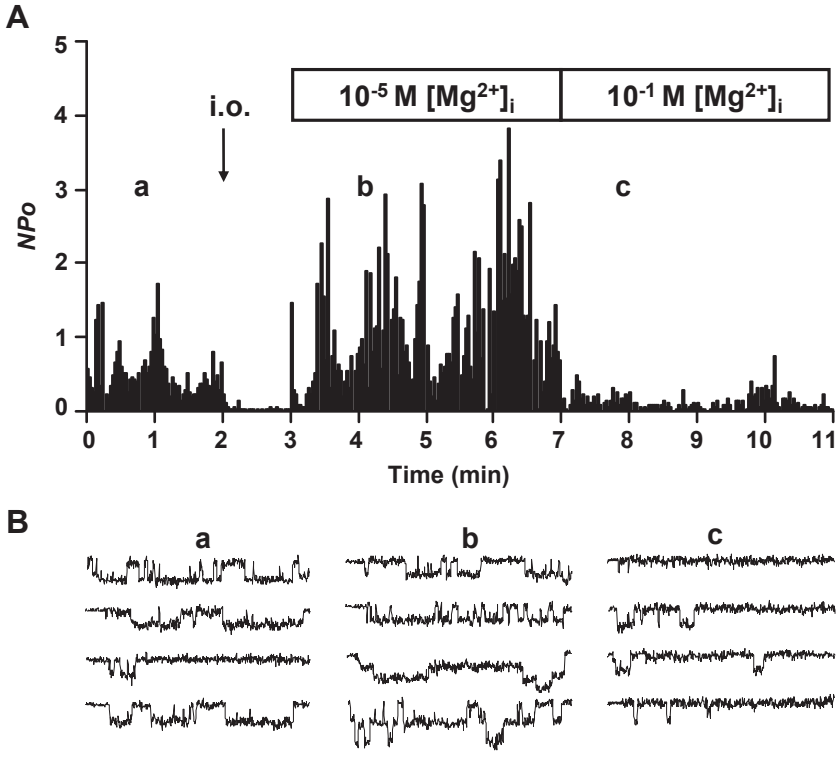

Fig. 3. Facilitatory and inhibitory effects of Mg^{2+} on L-type Ca^{2+} channels. The channel activity (*NPo*) of single L-type Ca^{2+} channels was recorded in the inside-out patch conformation. A: *NPo* of the channels was calculated for repetitive depolarization and plotted against time. The inside-out patch mode (i.o.) was initiated, as indicated by the arrow after a 2 min recording time of *NPo* in the cell-attached mode. Intracellular Mg^{2+} concentrations $[Mg^{2+}]_i$ of 10^{-5} M and 10^{-1} M were applied, together with CaM and ATP, as indicated by the boxes. B: Typical single-recording traces for the same experiment as in panel A, in the cell-attached mode (a), and with treatment with $[Mg^{2+}]_i$ of 10^{-5} M (b), and 10^{-1} M (c), recorded at the times indicated by the same letters in panel A.

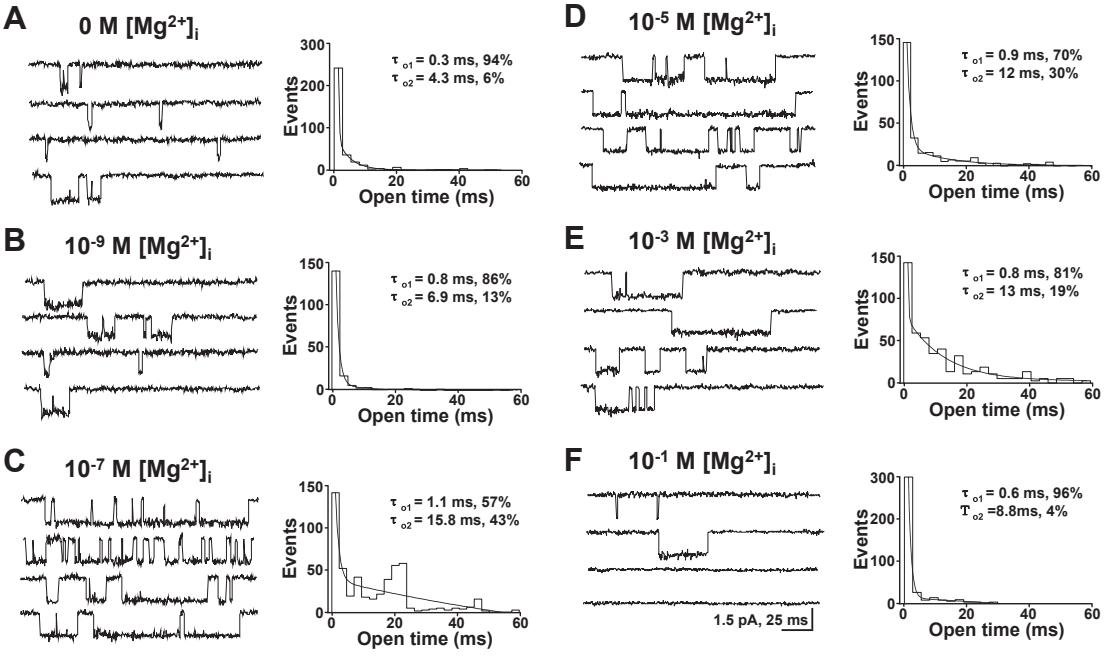

Fig. 4. Mg^{2+}-dependent regulation of the open time of single L-type Ca^{2+} channels. Open time histograms plotted for duration of open time, in bins, against the number of events. Open time distributions were best fit by the sum of two exponentials and the short (τ_{o1}) and long (τ_{o2}) time constants from these fits. Representative traces from inside-out patches at 0 mV and open time histograms for all open events from one patch for ventricular myocytes treated with intracellular Mg^{2+} concentrations $[Mg^{2+}]_i$ of 0 M (A), 10^{-9} M (B), 10^{-7} M (C), 10^{-5} M (D), 10^{-3} M (E), and 10^{-1} M (F) are shown.

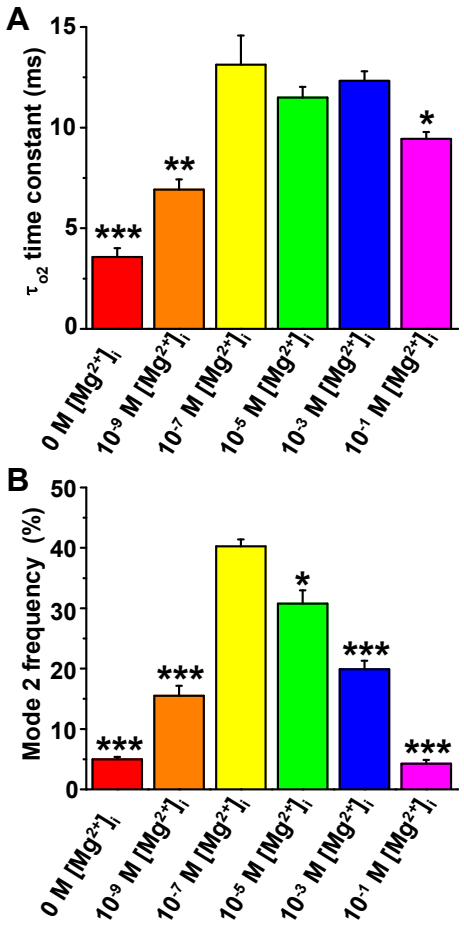

Fig. 5. Concentration-dependence of the Mg^{2+} effects on mode 2 gating of the Ca^{2+} channel. Summary of the values for the long open-time constants (τ_{o2}, ms) (A), as well as the frequency of mode 2 openings (τ_{o2}, %) (B) at an intracellular Ca^{2+} concentration $[Ca^{2+}]_i$ of 100 nM $^*P < 0.05$, $^{**}P < 0.01$, $^{***}P < 0.001$ compared with the 10^{-7} M intracellular Mg^{2+} concentration $[Mg^{2+}]_i$ group. $n = 3$.

instance, in the cell-attached mode used in Lansman's experiment, the ventricular myocyte was intact, and $[Mg^{2+}]_i$ was at physiological concentration of at least 0.3 mM.

In our study, we also found the Mg^{2+} induced inhibitory effects in Ca^{2+} channels at higher $[Mg^{2+}]_i$ (10^{-7} to 10^{-1} M). Previous studies referring to macroscopic Ca^{2+} current have also shown marked inhibitory effects of increased $[Mg^{2+}]_i$ (13,18,19,25). The study of $[Mg^{2+}]_i$ effects on L-type Ca^{2+} current (I_{Ca}) in frog ventricular myocytes showed that I_{Ca} was dramatically decreased by increasing $[Mg^{2+}]_i$ from 10^{-6} to 10^{-3} M at an intracellular Ca^{2+} concentration ($[Ca^{2+}]_i$) of 10^{-8} M (13,25). The inside-out single channel recoding method preserved the property of Mg^{2+} sensitivity, but the profile of this concentration dependence did not seem to be identical to that observed in the whole-cell recoding condition. We found that $[Mg^{2+}]_i$ between 10^{-7} and 10^{-1} M inhibited Ca^{2+} channel activity in a dose-dependent manner, using the inside-out configuration of the patch-clamp technique. The differences in the concentration-dependence profiles obtained using these two technique configurations may be due to the difference in their experimental conditions. For instance, in the cell-free patch condition, cytoplasmic proteins which might influence channel activity are absent.

Therefore, the concentration relationship for $[Mg^{2+}]_i$ from 0 to 10^{-1} M we obtained is bell-shaped. This relationship is similar to that exhibited for $[Ca^{2+}]_i$, that is explained by the well-known mechanisms of Ca^{2+}-dependent facilitation (CDF) and Ca^{2+}-dependent inactivation (CDI). Intracellular Mg^{2+} also appeared to have a dual effect on the L-type Ca^{2+} channels, which consisted of facilitation and inhibition. The underlying mechanism of CDF and CDI is well documented, which are mainly thought to be mediated by the binding of CaM as a Ca^{2+} sensor to the channel (1). However, the underlying mechanism of Mg^{2+}-induced facilitation and inactivation on Ca^{2+} channel activity has not yet been determined.

Since the facilitation effect of Mg^{2+} was first reported in the present study, we deduced the possible mechanism based on the reported literature on the inhibitory effect of Mg^{2+} on Ca^{2+} channel. Basically, direct or indirect effects could be considered. For the direct effect, Mg^{2+} may directly block the pore of the channel to inhibit the Ca^{2+} currents as suggested in Kuo and Hess's work with cultured pheochromocytoma cells (23). Meanwhile, recently it was suggested that the EF-hand motif region in the COOH-terminal tail of the α-subunit of the channel may be a direct binding site of Mg^{2+} to regulate the channel gating (18). For the indirect mechanisms, at least three possibilities could be considered. First, it was reported that increasing Mg^{2+} shifted both the I–V relationship and inactivation curve in a negative direction (16,34). Similar effects were also observed in our study in whole cell recording configuration in the range of $[Mg^{2+}]_i$ from 10^{-5} M to 10^{-1} M (data not shown). These effects might due to the altered surface charge shielding and/or a change in the kinetics of the V_m (membrane potential)-dependent gating process, suggesting that a shift in voltage-dependent inactivation might be one of the mechanisms to account for Mg^{2+}-dependent modulation of Ca^{2+} currents. Second, Mg^{2+} may regulate I_{Ca} through changing the phosphorylation level of the channel by kinase/phosphatase (13,19,24), or through influencing on the PIP_2 system by affecting PIP_2 synthesis and hydrolysis (35). Third, Mg^{2+} may possibly affect the Ca^{2+} dependent gating process of the channel activity (19).

The common point of the above mentioned possible mechanisms is that Mg^{2+} may modulate the channel gating kinetics. Based on our present results, we also propose that Mg^{2+} may affect the L-type Ca^{2+} channel gating kinetics to lead to Mg^{2+}-induced facilitation and inactivation of the channel activity. The L-type Ca^{2+} channels have been shown to demonstrate a modal behavior in the gating kinetics (31). The gating modes of mode 0, mode 1 and mode 2 are characterized with no opening, brief opening, and rarely appeared long-lasting opening (31), respectively. In the present study, by applying Bay K8644, the open-state probability of L-type Ca^{2+} channels was increased, and the mode 2 was promoted, which make it possible to observe the change of gating mode. Especially, a previous study conducted with whole-cell recording configuration showed that the effects of Mg^{2+} on L-type Ca^{2+} channels could be observed in both the presence and absence of Bay K8644 (17). After mode gating analysis, we found that mode 2 gating, but not mode 1 gating, is depended on the $[Mg^{2+}]_i$ in this experimental condition. Compared with Ca^{2+} channel activity in the absence of Mg^{2+}, the channel activity in the presence of lower $[Mg^{2+}]_i$ ($<10^{-7}$ M) was enhanced through increasing both the long open-time constant (τ_{o2}) and frequency of mode 2. Whereas, compared with the highest channel activity (occurring at 10^{-7} M Mg^{2+}), the channel activity in the presence of higher $[Mg^{2+}]_i$ ($\geq 10^{-5}$ M) was inhibited mainly via decreasing the frequency of mode 2, although the long open-time constant (τ_{o2}) was not change significantly. Thus, the modal shifts between the high open-probability state (mode 2) and the lower open-probability states (mode 1 and 0) may be involved in the mechanism of Mg^{2+} modulation of channel activity. This hypothesis is consistent with the findings of Yamaoka and Seyama (25) who reported that channel availability increased upon the lowering of cytosolic Mg^{2+} from millimolar to micromolar concentrations, reflecting the shift of channels from silent (mode 0) to

active (mode 1) modal states. Moreover, Wang et al. (17,19) and Catterall's group (14,15,18) also proposed a similar hypothesis based on their data.

Our results from the application of a series of $[Mg^{2+}]_i$, have shown that Mg^{2+} has a dual effect on the L-type Ca^{2+} channel activity: facilitation and inhibition. Lower $[Mg^{2+}]_i$ maintains and enhances the basal activity of Ca^{2+} channels, whereas higher $[Mg^{2+}]_i$ inhibits the channel activity. Therefore, Mg^{2+} may play important roles not only in physiological but also in pathophysiological processes. Thus, the observations of the present study are of significance for stimulating new ideas and developing new agents for the prevention and/or treatment of some related myocardial diseases. For example, Mg^{2+} may possibly be used as not only an agent to keep the basal activity of Ca^{2+} channels at certain level to maintain the cardiac function stable, but also an antagonist to alleviate Ca^{2+} toxicity in the treatment of cardiac diseases (2,36).

Conflict of interest

The authors declare that they have no conflict of interest.

Acknowledgments

This work was supported by grants from the National Natural Science Foundation of China (31471091).

References

(1) Hofmann F, Flockerzi V, Kahl S, Wegener JW. L-type Cav1.2 calcium channels: from in vitro findings to in vivo function. Physiol Rev. 2014;94:303–326.
(2) Bangalore S, Parkar S, Messerli FH. Long-acting calcium antagonists in patients with coronary artery disease: a meta-analysis. Am J Med. 2009;122:356–365.
(3) Gifford JL, Walsh MP, Vogel HJ. Structures and metal-ion-binding properties of the Ca^{2+}-binding helix-loop-helix EF-hand motifs. Biochem J. 2007;405:199–221.
(4) Yamamura H, Suzuki Y, Imaizumi Y. New light on ion channel imaging by total internal reflection fluorescence (TIRF) microscopy. J Pharmacol Sci. 2015;128:1–7.
(5) de Leon M, Wang Y, Jones L, Perez-Reyes E, Wei X, Soong TW, et al. Essential Ca^{2+}-binding motif for Ca^{2+}-sensitive inactivation of L-type Ca^{2+} channels. Science. 1995;270:1502–1506.
(6) Kolte D, Vijayaraghavan K, Khera S, Sica DA, Frishman WH. Role of magnesium in cardiovascular diseases. Cardiol Rev. 2014;22:182–192.
(7) Takaya J, Higashino H, Kobayashi Y. Can magnesium act as a second messenger? Current data on translocation induced by various biologically active substances. Magn Res. 2000;13:139–146.
(8) Li FY, Chaigne-Delalande B, Kanellopoulou C, Davis JC, Matthews HF, Douek DC, et al. Second messenger role for Mg^{2+} revealed by human T-cell immunodeficiency. Nature. 2011;475:471–476.
(9) Euser AG, Cipolla MJ. Magnesium sulfate for the treatment of eclampsia: a brief review. Stroke. 2009;40:1169–1175.
(10) Zhao L, Lou J, Wu H, Yin Y, Kang Y. Effects of taurine-magnesium coordination compound on ionic channels in rat ventricular myocytes of arrhythmia induced by ouabain. Biol Trace Elem Res. 2012;147:275–284.
(11) Standley CA, Batia L, Yueh G. Magnesium sulfate effectively reduces blood pressure in an animal model of preeclampsia. J Matern Fetal Neonatal Med. 2006;19:171–176.
(12) Coates BJ, Broderick TL, Batia LM, Standley CA. $MgSO_4$ prevents left ventricular dysfunction in an animal model of preeclampsia. Am J Obstet Gynecol. 2006;195:1398–1403.
(13) White RE, Hartzell HC. Effects of intracellular free magnesium on calcium current in isolated cardiac myocytes. Science. 1988;239:778–780.
(14) Brunet S, Scheuer T, Catterall WA. Increased intracellular magnesium attenuates beta-adrenergic stimulation of the cardiac Ca(V)1.2 channel. J Gen Physiol. 2013;141:85–94.
(15) Brunet S, Scheuer T, Catterall WA. Cooperative regulation of Ca(v)1.2 channels by intracellular Mg^{2+}, the proximal C-terminal EF-hand, and the distal C-terminal domain. J Gen Physiol. 2009;134:81–94.
(16) Wang M, Berlin JR. Voltage-dependent modulation of L-type calcium currents by intracellular magnesium in rat ventricular myocytes. Arch Biochem Biophys. 2007;458:65–72.
(17) Wang M, Berlin JR. Channel phosphorylation and modulation of L-type Ca^{2+} currents by cytosolic Mg^{2+} concentration. Am J Physiol Cell Physiol. 2006;291:C83–C92.
(18) Brunet S, Scheuer T, Klevit R, Catterall WA. Modulation of Cav1.2 channels by Mg^{2+} acting at an EF-hand motif in the COOH-terminal domain. J Gen Physiol. 2005;126:311–323.
(19) Wang M, Tashiro M, Berlin JR. Regulation of L-type calcium current by intracellular magnesium in rat cardiac myocytes. J Physiol. 2004;555:383–396.
(20) Buri A, McGuigan JA. Intracellular free magnesium and its regulation, studied in isolated ferret ventricular muscle with ion-selective microelectrodes. Exp Physiol. 1990;75:751–761.
(21) Hongo K, Konishi M, Kurihara S. Cytoplasmic free Mg^{2+} in rat ventricular myocytes studied with the fluorescent indicator furaptra. Jpn J Physiol. 1994;44:357–378.
(22) Yamaoka K, Kameyama M. Regulation of L-type Ca^{2+} channels in the heart: overview of recent advances. Mol Cell Biochem. 2003;253:3–13.
(23) Kuo CC, Hess P. Block of the L-type Ca^{2+} channel pore by external and internal Mg^{2+} in rat phaeochromocytoma cells. J Physiol. 1993;466:683–706.
(24) Pelzer S, La C, Pelzer DJ. Phosphorylation-dependent modulation of cardiac calcium current by intracellular free magnesium. Am J Physiol Heart Circ Physiol. 2001;281:H1532–H1544.
(25) Yamaoka K, Seyama I. Regulation of Ca channel by intracellular Ca^{2+} and Mg^{2+} in frog ventricular cells. Pflugers Arch. 1996;431:305–317.
(26) Xu JJ, Hao LY, Kameyama A, Kameyama M. Calmodulin reverses rundown of L-type Ca^{2+} channels in guinea pig ventricular myocytes. Am J Physiol Cell Physiol. 2004;287:C1717–C1724.
(27) Han DY, Minobe E, Wang WY, Guo F, Xu JJ, Hao LY, et al. Calmodulin- and Ca^{2+}-dependent facilitation and inactivation of the Cav1.2 Ca^{2+} channels in guinea-pig ventricular myocytes. J Pharmacol Sci. 2010;112:310–319.
(28) Chiang NJ, Wu SN, Chen LT. The potent activation of Ca(2+)-activated K(+) current by NVP-AUY922 in the human pancreatic duct cell line (PANC-1) possibly independent of heat shock protein 90 inhibition. J Pharmacol Sci. 2015;127:404–413.
(29) Kaibara M, Kameyama M. Inhibition of the calcium channel by intracellular protons in single ventricular myocytes of the guinea-pig. J Physiol. 1988;403:621–640.
(30) Sun Y, Xu J, Minobe E, Shimoara S, Hao L, Kameyama M. Regulation of the Cav1.2 cardiac channel by redox via modulation of CaM interaction with the channel. J Pharmacol Sci. 2015;128:137–143.
(31) Hess P, Lansman JB, Tsien RW. Different modes of Ca channel gating behaviour favoured by dihydropyridine Ca agonists and antagonists. Nature. 1984;311:538–544.
(32) Zhao M, Zhao J, He G, Sun X, Huang X, Hao L. Effects of astragaloside IV on action potentials and ionic currents in guinea-pig ventricular myocytes. Biol Pharm Bull. 2013;36:515–521.
(33) Lansman JB, Hess P, Tsien RW. Blockade of current through single calcium channels by Cd^{2+}, Mg^{2+}, and Ca^{2+}. Voltage and concentration dependence of calcium entry into the pore. J Gen Physiol. 1986;88:321–347.
(34) Hartzell HC, White RE. Effects of magnesium on inactivation of the voltage-gated calcium current in cardiac myocytes. J Gen Physiol. 1989;94:745–767.
(35) Wu L, Bauer CS, Zhen XG, Xie C, Yang J. Dual regulation of voltage-gated calcium channels by PtdIns(4,5)P2. Nature. 2002;419:947–952.
(36) Ioroi T, Akao M, Iguchi M, Kato M, Kimura T, Izumi Y, et al. Serofendic acid protects against myocardial ischemia-reperfusion injury in rats. J Pharmacol Sci. 2014;126:274–280.